Yang, B., Yang, E., Yu, L., & Niu, C. (2023).
Ultrasonic and IMU based high precision UAV localisation for the low cost autonomous inspection in oil and gas pressure vessels.
IEEE Transactions on Industrial Informatics, 1-12.
https://doi.org/10.1109/TII.2023.3240874

Ultrasonic and IMU Based High Precision UAV Localisation for the Low Cost Autonomous Inspection in Oil and Gas Pressure Vessels

Beiya Yang, *Graduate Student Member, IEEE*, Erfu Yang, *Senior Member, IEEE*, Leijian Yu, *Graduate Student Member, IEEE*
and Cong Niu, *Member, IEEE*

***Abstract*—With the increasing demands for unmanned aerial vehicle (UAV) based autonomous inspections in the oil and gas industry, one of the challenging issues for 3D UAV positioning has emerged due to the satellite signal blocking. Considering the existing characteristics of the ultrasonic based technique, such as the low cost, extremely lightweight and high positioning accuracy, it can be promising as the potential solution. Nevertheless, the low position update rate and vulnerable positioning performance to the changing environment still limit its applications on UAV. Therefore, in this article, an ultrasonic and inertial measurement unit (IMU) based localisation algorithm and low cost UAV autonomous inspection system are presented. With the incorporation of the IMU, the position update rate, accuracy and stability of the algorithm can all be significantly improved. This is done by the adaptively estimated noise covariance matrices through the proposed adaptive extended Kalman filter (AEKF) algorithm and the added weighting factors. Followed by, an additional virtual observation process is presented to overcome the unavailability of the observation information for further performance improvement. Finally, extensive numerical results and field tests demonstrate that the proposed algorithm and system can achieve the high update rate, reliable, accurate and precision UAV positioning in oil and gas pressure vessels and are feasible for the UAV autonomous inspection in these environments.**

***Index Terms*—3D Localisation, unmanned aerial vehicle (UAV), ultrasonic, inertial measurement unit (IMU), sensor fusion, autonomous inspection, oil and gas pressure vessels.**

I. Introduction

ALONG with the significant development of artificial intelligence (AI) and robotics, leveraging unmanned aerial vehicle (UAV) for the autonomous inspection becomes a new research area to meet the industrial needs [1], [2]. In the oil and gas industry, the periodic inspection is required for the pressure vessel utilised for the storage of the oil and gas to detect the cracks or corrosion. Traditionally, this work is carried out by the experienced engineers. However, considering the flammable and explosive characteristics of the oil and gas and the extremely confined space, it is unsafe and difficult for human to access. In addition, the dark environment inside the pressure vessel will also have the huge impact on the working efficiency and accuracy. Therefore, leveraging UAV for autonomous inspection turns into a potential solution [3], [4]. Currently, a commercial UAV named Elios 2 designed by Flyability has already been extensively used for the inspection in the oil and gas industry [5]. Nevertheless, Elios 2 can only be manually controlled by well-trained engineers, due to the lack of UAV position information in such environments. For traditional UAV applications, the precise position information of UAV can be provided by the global positioning system (GPS). But owing to the satellite signal blocking, it is impossible for GPS to provide this information. Instead of the precise UAV positioning, Elios 2 is mounted with a carbon fibre protection frame to prevent collision and only provide the manual mode for inspection. Thus, in order to realise the UAV based autonomous inspection in oil and gas pressure vessels, a new technology which can achieve the precise 3D localisation of UAV is required.

Accordingly, the precise UAV positioning is challenging and pressingly needed for the UAV based autonomous inspection. This appears to be particularly important for the applications in the oil and gas pressure vessels, which is the focused application under the consideration in this paper. The unsafe, difficult to access, dark, extremely confined and GPS-denied characteristics for the focused application all have the significant impact on the existing UAV based localisation techniques. As a result, in order to meet the industrial needs, the research on the precise UAV positioning in such environment to keep its stability for the autonomous inspection becomes an important and attractive area. Currently, different localisation techniques have already been investigated and applied for the precise UAV positioning to achieve the UAV based autonomous inspection in the similar environments. In [6], a smart UAV inspection system was designed for the application inside an industrial boiler. The precise UAV positioning was achieved through the integration of inertial measurement unit (IMU) or inertial navigation system (INS) and vision based approach. However, considering the dark and textureless environment, the localisation performance for vision based approaches will be influenced. Differently, authors in [7] and [8] from the same research group proposed a deep learning based direction identification approach for micro aerial vehicle (MAV) inspection inside a mining tunnel. Instead of the precise localisation, the images captured by the on-board camera were exploited for heading direction identification to prevent collision. Nevertheless, they considered the MAV as a free-flying object, only the heading

The authors are within the Department of Design, Manufacturing and Engineering Management, University of Strathclyde, 75 Montrose Street, Glasgow G1 1XJ, UK. The corresponding author is Dr. Erfu Yang. (email: beiya.yang@strath.ac.uk, erfu.yang@strath.ac.uk, leijian.yu@strath.ac.uk, cong.niu@strath.ac.uk)

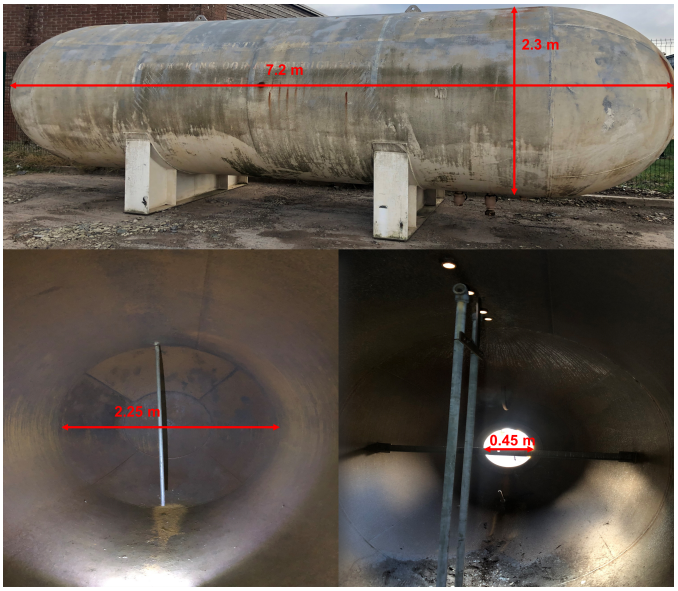

Fig. 1. Oil and gas pressure vessel.

direction was provided. For the focused application, known as the extremely confined space, with only the heading direction information, the MAV or UAV may crash. Apart from vision based techniques, localisation approaches based on light detection and ranging (LiDAR) techniques have also been widely applied for UAV positioning, due to the robust performance in the dark and textureless environments. Authors in [9] achieved the precise UAV positioning in dark areas of large historical monuments with the easy-to-obtain 3D point cloud and 2D LiDAR. However, how to generate the precise point cloud in the difficult access space will be a problem. Ozaslan et al. [10], [11] designed a MAV based autonomous navigation and mapping system for the autonomous inspection of penstocks and tunnels leveraging the integration of LiDAR, IMU and vision. Yet, the high energy consumption of the LiDAR system will have the huge impact on the operation time of MAV, and the system cost needs to be considered. Mansouri et al. [12] proposed another autonomous navigation approach for MAV in dark underground mine environment with the utilisation of the optical flow and 2D LiDAR. Instead of localisation, they were more focused on the direction identification. Nevertheless, the completely dark environment still has the influence on the localisation performance of optical flow, and the energy consumption of the 2D LiDAR still needs to be taken into account. Furthermore, due to the weight of the LiDAR system, a relatively large UAV like DJI F550 is required to carry all the components. However, considering the focused application has the extremely confined space as shown in Fig. 1 (2.25m $\times$ 7.2m $\times$ 2.3m, entrance: 0.45m). It is still infeasible to utilise the UAV studied in the aforementioned literature. Thus, a low cost, extremely lightweight and high accuracy localisation technique for UAV positioning is still needed.

Considering the low cost, extremely lightweight and high accuracy requirements, the ultrasonic based localisation technique can be promising as the potential solution [13]. Currently, the ultrasonic sensor has already been widely utilised on UAV systems for target detection, structure inspection, smart navigation and collision avoidance [14]–[16]. One of the typical representative commercial solutions can be the system designed by Marvelmind [17], lots of relevant researches have already been carried out with this commercial system. Kang et al. [18] proposed an autonomous UAV system with the ultrasonic localisation system for the structural health monitoring. Li et al. [19] employed the ultrasonic system for UAV navigation in indoor environment. Zahran et al. [20] even utilised the ultrasonic localisation system to serve as the ground truth for performance evaluation. Nevertheless, the ultrasonic based localisation technique still have its shortcomings, which may greatly limit its applications on UAV. Firstly, it is impossible to provide a high position update rate in terms of the propagation speed for the acoustic wave. For Marvelmind, they declared that the position update rate or ranging update rate for their system is up to 25Hz [17] in the ideal case. The position update rate is known as one of the key performance indicators (KPIs) to evaluate the performance of the UAV positioning system [21]. It has the great influence on the stability of the UAV. Secondly, the noises come from the propellers may cause the appearance of the unreasonable value within the ranging information and lead to the positioning performance oscillation as seen from the experiment results. Thirdly, the acoustic wave is vulnerable to the operational environment variation. Fourthly, during the operational process, the unavailability of the observation information always exists. This unavailability will directly cause the positioning failure or performance degradation. These all may lead to the instability of UAV.

To remedy the aforementioned issues, the investigation on the Kalman filter (KF) based sensor fusion approaches has been carried out. This is due to the implementation simplicity, high position update rate, and high precision performance characteristics of these approaches [22]. To overcome the problem of low position update rate and limits the performance influence of the unreasonable value within the ranging information. Guo et al. [23] and Li et al. [24] all proposed the extended Kalman filter (EKF) based sensor fusion approach plus with the measurements calibration and outlier detection methods. Especially for [24], the additional angular rate is considered in the prediction process to enhance the accuracy of the orientation information for positioning performance improvement. However, the requirement of the reference points (points with known position information) in the system runs counter to the applications in hardly access environments. The error accumulation caused by the unavailability of the ranging information also has the huge impact on the localisation performance of these approaches with the ultrasonic system. To deal with the problem of the unavailability of the observation information, in [25], a virtual sensor called sliding-mode observer (SMO) and a hybrid global estimator (HGE) are proposed and constructed. In their approach, firstly, more vehicle states are estimated by SMO and provided to HGE to serve as the partial observation information. Then, the grey predictor (GP) is exploited to predict the behavior of the strap-down inertial navigation system (SINS) through the limited data for performance enhancement. However, the positioning performance for UAV applications in focused environments is

still limited due to the added computational complexity and the large accumulation error from IMU. From the different perspective, authors in [26] proposed a self-learning square-root-cubature Kalman filter (SL-SRCKF) approach to overcome the GPS outage issue. Instead of predicting the position error from the SINS, the long short-term memory (LSTM) neural network is used to learn the relationship between the predicted state vector and the observation information. Through this learned relationship, the prediction for the observation information can be made during the outage period. Different from [25], the positioning error led by the noise from IMU can be limited by [26]. Nevertheless, the increased computational complexity and the additional training process will limit the position update rate and restrict the applications on UAV. Furthermore, as declared, the training time required for LSTM is roughly 129s once, which means a long-term accurate observation information is desired for training propose. Yet, the unreasonable value and the unavailability of the ranging information always exist in the operation of the ultrasonic positioning system. Meanwhile, it is difficult to capture enough data for training during the flight of UAV. These all limit its applications on UAV positioning with ultrasonic system. In addition, one critical issue never considered for all the aforementioned approaches is the influence of the unknown and changing noise covariance matrices. This appears to be particularly important for UAV applications, because the propagation condition and operational environment are time-varying during the flight of UAV. The process and measurement noise covariance matrices highly affect the performance and stability of the positioning system [27], inappropriate noise covariance matrices may even lead to the filtering divergence [28]. To deal with this issue, an additional trial and error tuning process is often required to find the appropriate noise covariance matrices [27]. However, it may cost lot of time and greatly limit the system application scenarios. Unlike the traditional applications, in the focused oil and gas pressure vessel environments, the operational space for the UAV is extremely confined and it is difficult for human to access. As a result, it is difficult to adjust the noise covariance matrices through trial and error. Furthermore, to keep the stability of UAV in such environments and increase the operational time of UAV for the detailed inspection, the computational complexity and implementation simplicity of the approach also need to be considered. To solve all the existing issues under the focused applications, the adaptive extended Kalman filter (AEKF) becomes a more efficient technique [29]. Its advantages include the ability to adaptively estimate the noise covariance matrices, low computational complexity, implementation simplicity and less prior information requirement [30]. With all these merits, the reliable, accurate, high update rate and low computational complexity positioning of the UAV in the focused environments can be achieved.

In order to remedy the aforementioned issues for reliable, accurate, high position update rate and low computational complexity 3D UAV localisation to achieve autonomous inspection in oil and gas pressure vessels, an ultrasonic and IMU based UAV autonomous inspection system is firstly proposed. The main contributions of this article are listed as follows:

1) An ultrasonic and IMU based sensor fusion approach is proposed, focusing on the precise 3D UAV localisation in oil and gas pressure vessels. With the additional IMU, the adaptively estimated noise covariance matrices and the added weighting factors for the estimation of these matrices, the approach can significantly improve the UAV positioning performance and increase the position update rate with low computational complexity to keep the stability of UAV in such environments.
2) A virtual observation process is proposed and applied in the system to eliminate the performance degradation caused by the operational environment variation and the noises from the propellers to keep the stability of the UAV in such environments and overcome the observation information unavailability problem.
3) An ultrasonic and IMU based UAV autonomous inspection system is developed and implemented for the autonomous inspection inside oil and gas pressure vessels.

The remainder of the article is organised as follows. Section II gives an overview of the whole UAV based autonomous inspection system. Section III presents an introduction and discussion about the ultrasonic and IMU based sensor fusion approach for UAV positioning. To comprehensively prove the effectiveness of the proposed algorithm and system, laboratory experiments and field tests are carried out in Section IV. Finally, the conclusion is made in Section V.

II. System Overview

The structure of the UAV based autonomous inspection system is depicted in Fig. 2. The system consists of five modules, including the UAV, ground station, localisation module, recording module and illumination module. Considering the size, weight and cost of the system, the Bebop 2 developed by Parrot is selected in the system. The ground station is a laptop with Intel(R) Core(TM) i7-8750H CPU, responsible for the UAV position determination, control command generation and transmission. The localisation module is composed of two parts, i.e., the ultrasonic sensor nodes and the IMU. Throughout the communication between the anchor nodes (auxiliary nodes with known positions) and tag node (equipped on the UAV), the distance information between these ultrasonic sensor nodes can be estimated and transmitted to the ground station. The IMU attached on the UAV is exploited to provide the acceleration and orientation information of UAV and transmit to the ground station for position estimation. In order to illuminate the whole area and provide high quality images and videos for precise inspection, the illumination module and recording module are added on the UAV. The Insta360 GO 2 is utilised as the recording component due to the tiny size, lightweight and high performance features. The illumination module is composed of three torches, including one central torch – Olight Baton 3 to light the dark environment inside the pressure vessel and two mini torches – Olight i1R 2 EOS to illuminate the ground. All the components attached on the UAV can power themselves with their own batteries. The detailed information for each component is summarised in Table I. Within these, since the ultrasonic modem is not

TABLE I
TECHNICAL PARAMETERS AND PRICE FOR EACH COMPONENT.

Name	Number	Price (£)	Size (mm)	Weight (g)	Additional Notes
Parrot Bebop 2	1	279.99	381 × 327.7 × 88.9	504	N/A
Ultrasonic Sensor	5	60.7	55 × 55 × 67	59	N/A
Ultrasonic Modem	1	60.7	N/A	N/A	N/A
IMU (BNO055)	1	26	20 × 27 × 4	3	N/A
Insta 360 go 2	1	294.99	52.9 × 23.6 × 20.7	26.5	2560x1440 50fps, FlowState stabilisation
Olight Baton 3	1	51.96	63 × 21 × 21	53	1200 Lumens
Olight i1R 2 EOS	2	12.57	44 × 14.8 × 14.8	13.5	150 Lumens

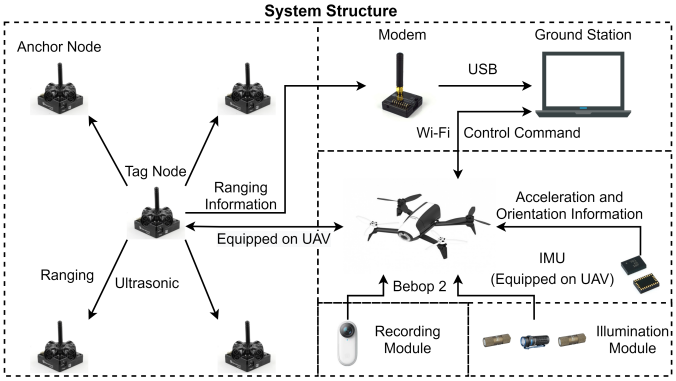

Fig. 2. System structure.

mounted on the UAV, the size and weight for the ultrasonic modem are not considered.

During the operational process of the whole system, firstly, the acceleration and orientation information from the IMU module are transmitted to the ground station. Simultaneously, the time of departure (TOD) and time of arrival (TOA) for the communication between the ultrasonic sensor equipped on the UAV (tag node) and the fixed ultrasonic sensor nodes (anchor nodes) are all transmitted to the ultrasonic modem for distance calculation, and then sent to the ground station. The ground station is responsible for the position estimation through the recorded acceleration, orientation and distance information. The flight path of the UAV in the system is prepared before the flight of UAV and recorded in the ground station. Finally, with the flight path and estimated position information, the control command will be generated and transmitted to the UAV through the ground station to complete the tasks.

III. SENSOR FUSION BASED UAV POSITIONING

According to the system overview, one of the most important information for this UAV based autonomous inspection system is the position information of UAV. However, as aforementioned, with the pure ultrasonic based localisation technique, the localisation performance and stability of UAV are greatly influenced by the low position update rate, variation of the operational environment and the noises come from the propellers. In order to remedy these existing issues, in this section, the ultrasonic and IMU based sensor fusion approach is introduced.

A. Transformation of the coordinate frame

It is noted that all the required information including the acceleration, orientation and position information are within different coordinate frames. In order to appropriately depict the UAV's attitude, and estimate the accurate position information, a suitable coordinate frame is firstly required. Different from traditional applications, a relative navigation frame can be defined by the fixed anchor nodes in the system. Therefore, the conversion between the IMU coordinate frame and the relative navigation frame is sufficient.

In order to make the transformation process more intuitive, the Euler angle is selected to present the whole conversion process. The three Euler angles (roll, pitch and yaw) between these two frames are assumed as ϕ, θ and ψ. Then the transformation equation can be represented as

$$\boldsymbol{a}^{RN} = \boldsymbol{C}_{YRN}\boldsymbol{C}_{PY}\boldsymbol{C}_{IP}\boldsymbol{a}^{IMU}, \tag{1}$$

in which, $\boldsymbol{a}^{IMU}$ and $\boldsymbol{a}^{RN}$ are supposed as the acceleration information in the IMU frame and relative navigation frame, $\boldsymbol{C}_{IP}$, $\boldsymbol{C}_{PY}$ and $\boldsymbol{C}_{YRN}$ are denoted as the transformation matrix in each process to be expressed as

$$\boldsymbol{C}_{IP} = \begin{bmatrix} 1 & 0 & 0 \\ 0 & \cos\phi & -\sin\phi \\ 0 & \sin\phi & \cos\phi \end{bmatrix}, \tag{2}$$

$$\boldsymbol{C}_{PY} = \begin{bmatrix} \cos\theta & 0 & \sin\theta \\ 0 & 1 & 0 \\ -\sin\theta & 0 & \cos\theta \end{bmatrix}, \tag{3}$$

$$\boldsymbol{C}_{YRN} = \begin{bmatrix} \cos\psi & -\sin\psi & 0 \\ \sin\psi & \cos\psi & 0 \\ 0 & 0 & 1 \end{bmatrix}. \tag{4}$$

B. Sensor fusion based positioning

With the converted acceleration information and the kinematic model, the state prediction equation can be derived as

$$\begin{cases} \hat{\boldsymbol{u}}_{i/i-1} = \boldsymbol{u}_{i-1} + \Delta t \boldsymbol{v}_{i-1} + \frac{\Delta t^2}{2}\boldsymbol{a}_{i-1}^{RN} \\ \hat{\boldsymbol{v}}_{i/i-1} = \boldsymbol{v}_{i-1} + \Delta t \boldsymbol{a}_{i-1}^{RN} \\ \boldsymbol{a}_{i-1}^{RN} = \tilde{\boldsymbol{a}}_{i-1}^{RN} + \boldsymbol{\gamma}_{i-1}, \end{cases}, \tag{5}$$

where, the subscript i for all the variables denotes the number of the estimation round, $\hat{\boldsymbol{u}}_{i/i-1}$ is the predicted position of the UAV, $\hat{\boldsymbol{v}}_{i/i-1}$ is the predicted velocity of the UAV, $\boldsymbol{u}_{i-1} = [x_{i-1}, y_{i-1}, z_{i-1}]^T$ is the position of the UAV in the $i-1$ round, $\boldsymbol{v}_{i-1} = [v_{x,i-1}, v_{y,i-1}, v_{z,i-1}]^T$ is the velocity of

the UAV at each direction in the $i-1$ round, Δt represents the time interval between two rounds IMU measurements, $\boldsymbol{a}_{i-1}^{RN} = [a_{x,i-1}^{RN}, a_{y,i-1}^{RN}, a_{z,i-1}^{RN}]^T$ denotes the measured and converted acceleration in the $i-1$ round, $\tilde{\boldsymbol{a}}_{\boldsymbol{i-1}}{}^{RN}$ is the true value of the acceleration in the $i-1$ round and $\boldsymbol{\gamma}_{i-1}$ represents the IMU measurement noise in the $i-1$ round, assumed as the additive white Gaussian noise (AWGN) with zero mean and $\boldsymbol{Q}_\gamma$ covariance. Meanwhile, the declaration requires to be made that, considering the high update rate for the IMU measurements, the acceleration between two rounds measurements is supposed as constant. Then, converting these equations into matrix form yields

$$\hat{\boldsymbol{\rho}}_{i/i-1} = \boldsymbol{F}_i \boldsymbol{\rho}_{i-1} + \boldsymbol{B}_i \boldsymbol{a}_{i-1}^{RN}, \tag{6}$$

in which, $\boldsymbol{\rho}_{i-1} = [x_{i-1}, v_{x,i-1}, y_{i-1}, v_{y,i-1}, z_{i-1}, v_{z,i-1}]^T$ represents the state vector in the $i-1$ round constitutes by the position and velocity information, $\hat{\boldsymbol{\rho}}_{i/i-1}$ denotes the predicted state vector, $\boldsymbol{F}_i$ and $\boldsymbol{B}_i$ are assumed as the state transition matrix and control matrix in the i round,

$$\boldsymbol{F}_i = \boldsymbol{I}_3 \otimes \begin{bmatrix} 1 & \Delta t \\ 0 & 1 \end{bmatrix}, \tag{7}$$

$$\boldsymbol{B}_i = \boldsymbol{I}_3 \otimes \begin{bmatrix} \frac{\Delta t^2}{2} \\ \Delta t \end{bmatrix}. \tag{8}$$

Within the equation, $\boldsymbol{I}_3$ denotes the 3×3 identity matrix, "$\otimes$" represents the Kronecker product. Therefore, the state covariance matrix can be calculated

$$\hat{\boldsymbol{P}}_{i/i-1} = \boldsymbol{F}_i \boldsymbol{P}_{i-1} \boldsymbol{F}_i^T + \boldsymbol{Q}_i, \tag{9}$$

in which, $\boldsymbol{P}_{i-1}$ represents the previous state covariance matrix in the $i-1$ round, $\boldsymbol{Q}_i$ is regarded as the process noise covariance. Throughout the state prediction process, the position information of the UAV can be predicted. However, to get rid of the error accumulation comes from the IMU measurements, an additional correction process is still required.

In order to address this, the ranging information measured by the ultrasonic sensor nodes is exploited. Here, the observation matrix in the i round is supposed as $\boldsymbol{D}_i$. Then, the observation model can be built

$$\boldsymbol{D}_i = \boldsymbol{H}_i \hat{\boldsymbol{\rho}}_{i/i-1} + \boldsymbol{\omega}_i. \tag{10}$$

In the above equation, $\boldsymbol{\omega}_i$ is regarded as the measurement noise from ultrasonic sensor nodes in the i round, modelled as AWGN with zero mean and $\boldsymbol{Q}_{\omega_i}$ covariance. $\boldsymbol{H}_i$ represents the observation transition matrix in the i round,

$$\boldsymbol{H}_i = \begin{bmatrix} \frac{\partial d_{1,i/i-1}}{\partial \hat{x}_{i/i-1}} & 0 & \frac{\partial d_{1,i/i-1}}{\partial \hat{y}_{i/i-1}} & 0 & \frac{\partial d_{1,i/i-1}}{\partial \hat{z}_{i/i-1}} & 0 \\ \frac{\partial d_{2,i/i-1}}{\partial \hat{x}_{i/i-1}} & 0 & \frac{\partial d_{2,i/i-1}}{\partial \hat{y}_{i/i-1}} & 0 & \frac{\partial d_{2,i/i-1}}{\partial \hat{z}_{i/i-1}} & 0 \\ \vdots & \vdots & \vdots & \vdots & \vdots & \vdots \\ \frac{\partial d_{n,i/i-1}}{\partial \hat{x}_{i/i-1}} & 0 & \frac{\partial d_{n,i/i-1}}{\partial \hat{y}_{i/i-1}} & 0 & \frac{\partial d_{n,i/i-1}}{\partial \hat{z}_{i/i-1}} & 0 \end{bmatrix}, \tag{11}$$

which is approximated through the first order Taylor expansion, due to the non-linearity of it. Within it, $d_{n,i/i-1} = \left\| \boldsymbol{u}_n - \hat{\boldsymbol{u}}_{i/i-1} \right\|$ denotes the calculated distance information between the ultrasonic tag node and fixed anchor nodes through the predicted state information, n represents the number of fixed anchor nodes in the system.

TABLE II
RANGING RESULTS BETWEEN TAG NODE AND ANCHOR NODES.

Anchor 1 (m)	Anchor 2 (m)	Anchor 3 (m)	Anchor 4 (m)
1.637	1.774	1.687	1.828
1.638	1.735	1.698	1.817
1.612	6.145	1.721	1.795
1.617	1.744	1.711	7.366
1.622	1.628	1.694	1.792
1.654	1.729	1.708	1.789
1.619	1.729	1.728	1.801
1.645	1.721	1.757	1.769
1.651	5.827	1.764	1.814
1.641	1.704	1.766	1.041
1.615	1.673	0.6	1.74
1.667	1.67	1.812	1.756
1.654	8.017	1.847	1.813
1.715	1.579	1.84	1.735

Then, the Kalman gain at this round can be calculated and expressed as

$$\boldsymbol{K}_{i,Kalman} = \hat{\boldsymbol{P}}_{i/i-1} \boldsymbol{H}_i^T (\boldsymbol{H}_i \hat{\boldsymbol{P}}_{i/i-1} \boldsymbol{H}_i^T + \boldsymbol{R}_i)^{-1}, \tag{12}$$

where, $\boldsymbol{R}_i$ is assumed as the measurement noise covariance matrix in the i round which determined by the measurement noise $\boldsymbol{\omega}_i$ comes from the ultrasonic sensor nodes.

Finally, the predicted information from the state prediction process can be updated and corrected for performance improvement and preventing the error accumulation. However, due to the inherent nature of the acoustic wave, the huge performance oscillation caused by the variation of the operational environment and the noises come from the propellers still exists. This has the great impact on the stability of the UAV, especially for the applications inside the small oil and gas pressure vessels. To remedy the existing issues, a virtual observation process and an AEKF based sensor fusion approach are proposed and introduced as follows.

C. Virtual observation

Compared with other localisation techniques, the ultrasonic based technique is more likely to be influenced by the variation of the operational environment and the noises from the propellers, due to the inherent nature of the acoustic wave. In the localisation or ranging process, this influence may lead to a huge oscillation for the localisation or ranging results and may even lead to the unavailability of the ranging information.

As shown in Table II, the data for the ranging results from the ultrasonic sensor nodes captured during the flight of UAV are listed. Apparently from the ranging results, the huge oscillation for the measured distance can be observed. When looking at the results of anchor 2, the measured distance suddenly changed from 1.735m to 6.145m and recovered in the next round measurement. The same phenomenon can also be observed for other anchor nodes. These unreasonable values caused by the variation of the operational environment and the noises from the propellers may lead to the localisation performance oscillation or even the divergence of the filter.

According to the data captured, the standard deviation (STD) for the accuracy of the ranging information is greatly influenced by these unreasonable values which increased to 2.086m from 0.026m with no unreasonable values.

Furthermore, owing to the low propagation speed of the acoustic wave, the position or ranging update rate is extremely limited for the ultrasonic based localisation technique. According to the experiments results, the ranging update rate for the ultrasonic based system is around 16Hz in the ideal case for the focused applications. However, considering the variation of the operational environment which may lead to the unavailability of the ranging information and the existing unreasonable values, the ranging information can be provided to correct the results even after 30 rounds state perdition, in the extreme case. Under such circumstance, the accumulation error from the state prediction process will have the huge impact on the localisation performance and may cause the UAV crashes, especially under the focused application scenarios.

To remedy the aforementioned issues, a virtual observation process is proposed and introduced. For the focused application, considering the space is extremely confined a nd the speed of the UAV requires to be limited for safety reason. In addition, since the system is developed for the autonomous inspection in such environments, in order to keep a high image and video quality for detailed inspection, the speed of the UAV also needs to be limited. Under such circumstances, in our system, the speed of UAV in all directions are limited within 0.2m/s. Therefore, it can be supposed that, within a short time period, the UAV is relatively static. Taking all the existing factors into account, the following strategy is proposed

$$\begin{cases} \boldsymbol{D}_i = \boldsymbol{D}_{i,observed} & k <= k_{threshold} \\ \boldsymbol{D}_i = \begin{bmatrix} \|\boldsymbol{u}_1 - \hat{\boldsymbol{u}}_{i-1}\| \\ \|\boldsymbol{u}_2 - \hat{\boldsymbol{u}}_{i-1}\| \\ \vdots \\ \|\boldsymbol{u}_n - \hat{\boldsymbol{u}}_{i-1}\| \end{bmatrix}_{n\times 1} & k > k_{threshold} \end{cases}, \tag{13}$$

where, k represents the state prediction round number which is set as zero initially, $k_{threshold}$ is an added threshold value. During the localisation process, if the current prediction round number k exceeds $k_{threshold}$, the virtual observation value will be simulated and calculated through the previously estimated position information of the UAV and the prediction round number k will be set as zero in the next round. Otherwise, the observed ranging information will be utilised. In the virtual observation process, the threshold should be carefully selected. A larger $k_{threshold}$ means more trust on the predicted results, which may lead to the performance degradation caused by the error accumulation. This can directly lead to the drop-off for the performance of the system and cause the instability of the UAV inside the oil and gas pressure vessels. On the contrary, a smaller $k_{threshold}$ means much more virtual observation information will be provided. This will certainly lead to the accuracy drop-off due to the movement of UAV during the estimation process. The accuracy of the UAV position is directly linked to whether the UAV can hit the target point or not, which will have a great impact on the inspection accuracy and may lead to the crash. Furthermore, each distance measurement will be compared with the previous measurements. If a suddenly changed measurement is detected, the virtual observation value will also be simulated and utilised as the observation information in this round.

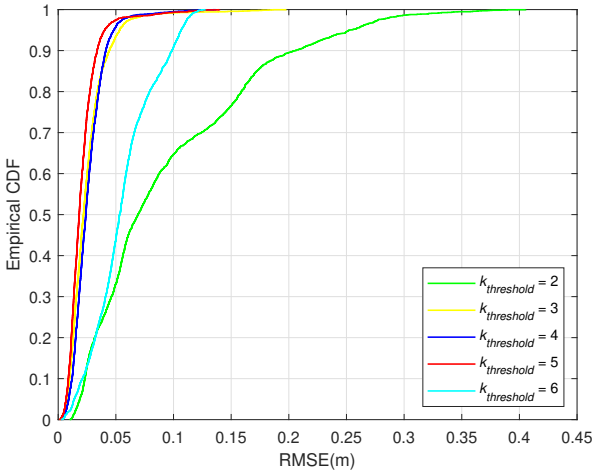

Fig. 3. eCDF results with different threshold values.

TABLE III
SIMULATION RESULTS WITH DIFFERENT THRESHOLD VALUES

$k_{threshold}$	Median Error (m)	95^{th} Error (m)	STD (m)
$k_{threshold}$ = 2	0.069	0.254	0.075
$k_{threshold}$ = 3	0.022	0.053	0.018
$k_{threshold}$ = 4	0.024	0.048	0.014
$k_{threshold}$ = 5	**0.018**	**0.040**	**0.014**
$k_{threshold}$ = 6	0.053	0.107	0.027

In order to find the suitable $k_{threshold}$ before the actual flight test, the simulations have been carried out in Gazebo environment. Here, to conform the anchor nodes can be deployed without human entering the pressure vessel, all the fixed anchor nodes are set on the same plane near the entrance of the oil and gas pressure vessel. The flight path of UAV is set as a reverse "S". Five different values of $k_{threshold}$ have been tested in the simulations. The empirical cumulative distribution function (eCDF), root mean square error (RMSE) and detailed simulation results have been provided in Fig. 3 and Table III.

Obviously from the simulation results, when being with smaller $k_{threshold}$ ($k_{threshold}$ = 2), a huge performance degradation with 0.069m median error, 0.254m 95^{th} error and 0.075m average STD can be observed. With the augmentation of the $k_{threshold}$, this performance degradation can be eased, due to the lesser virtual observation information in the estimation process. However, when being with a larger $k_{threshold}$ ($k_{threshold}$ = 6), the performance drop-off can still be observed which is led by the accumulation error from the prediction process. Finally, throughout the simulation, a suitable threshold value ($k_{threshold}$ = 5) is selected for the actual flight test considering the best performance with the median error, 95^{th} error and average STD to be 0.018m, 0.040m and 0.014m, respectively.

D. Noise covariance matrices estimation

Even the localisation performance can be improved with the aforementioned EKF based sensor fusion approach and the additional virtual observation process. The unknown noise covariance matrices will still limit the system performance. Besides, it is time consuming to adjust these matrices. Particularly, the actual noise covariance matrices are constantly changing due to the variation of the operational environment. Therefore, the AEKF based sensor fusion approach which is able to adaptively estimate the noise covariance matrices is investigated [31]–[33].

With the predicted position information and the observed distance information from the ultrasonic sensor nodes, the innovation covariance matrix $\hat{\boldsymbol{G}}_{\boldsymbol{D}_i'}$ can be obtained as

$$\hat{\boldsymbol{G}}_{\boldsymbol{D}_i'} = \frac{1}{M} \sum_{j=i-M+1}^{i} \boldsymbol{D}_j' \boldsymbol{D}_j'^{T}, \tag{14}$$

$$\boldsymbol{D}_i' = \boldsymbol{D}_i - \boldsymbol{H}_i \hat{\boldsymbol{\rho}}_{i/i-1}, \tag{15}$$

in which, $\boldsymbol{D}_i'$ represents the difference between the observed and predicted distance information in the i round, M is the window size or sampling number. Consequently the $\boldsymbol{R}_i$ matrix can be estimated

$$\boldsymbol{R}_i = \hat{\boldsymbol{G}}_{\boldsymbol{D}_i'} - \boldsymbol{H}_i \hat{\boldsymbol{P}}_i \boldsymbol{H}_i^T. \tag{16}$$

Similar to the estimation of the $\boldsymbol{R}_i$ matrix, the $\boldsymbol{Q}_i$ matrix can be approximated through the difference between the final corrected and predicted results at the same round. The difference can be expressed as

$$\begin{aligned} \boldsymbol{B}_i \boldsymbol{\gamma}_i &= \hat{\boldsymbol{\rho}}_i - \hat{\boldsymbol{\rho}}_{i/i-1} \\ &= \boldsymbol{K}_{i,Kalman} (\boldsymbol{D}_i - \boldsymbol{H}_i \hat{\boldsymbol{\rho}}_{i/i-1}) \end{aligned}. \tag{17}$$

Therefore, the $\boldsymbol{Q}_i$ matrix can be derived

$$\begin{aligned} \boldsymbol{Q}_i &= \boldsymbol{K}_{i,Kalman} E[\boldsymbol{D}_i' \boldsymbol{D}_i'^{T}] \boldsymbol{K}_{i,Kalman}^T \\ &= \boldsymbol{K}_{i,Kalman} \hat{\boldsymbol{G}}_{\boldsymbol{D}_i'} \boldsymbol{K}_{i,Kalman}^T \end{aligned}. \tag{18}$$

With the estimated noise covariance matrices, the performance degradation led by the environment variation can be further improved. Nevertheless, since the estimated noise covariance matrices are constantly changing, the filtering divergence is more likely to occur. This will certainly cause a crash. To solve this issue, the offline estimation results for the noise covariance matrices and two weighting factors α and β are utilised and added. Here it needs to note that, these two added offline estimation results of the noise covariance matrices $\boldsymbol{R}_{off}$ and $\boldsymbol{Q}_{off}$ are estimated before the flight of UAV, with the UAV statically at fixed point.

$$\boldsymbol{R}_i = (1-\alpha)\boldsymbol{R}_{off} + \alpha(\hat{\boldsymbol{G}}_{\boldsymbol{D}_i'} - \boldsymbol{H}_i \hat{\boldsymbol{P}}_i \boldsymbol{H}_i^T), \tag{19}$$

$$\boldsymbol{Q}_i = (1-\beta)\boldsymbol{Q}_{off} + \beta(\boldsymbol{K}_{i,Kalman} \hat{\boldsymbol{G}}_{\boldsymbol{D}_i'} \boldsymbol{K}_{i,Kalman}^T). \tag{20}$$

As seen from the above equations, the estimation of the noise covariance matrices is limited by the offline estimation results and these two weighting factors. It can be observed that with the increasing of the α or β, the estimation of the noise covariance matrices will give more trust on the current measurements to catch up the changes. However, this may cause the filtering divergence. On the contrary, with smaller weighting factors, a more stable estimation of the noise covariance matrices can be obtained. Nevertheless, there will be a performance degradation due to the inappropriate noise covariance matrices. Thus, the suitable weighting factors are required due to the connection with the positioning performance.

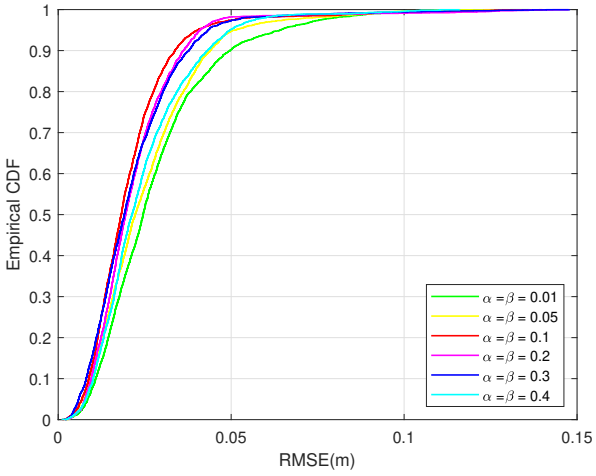

Fig. 4. eCDF results with different weighting factors.

In order to decide the suitable weighting factors, the simulations with different weighting factors for the proposed algorithm have been conducted. Similarly, the deployment strategy for fixed anchor nodes in the system and the planned path for the UAV are the same as the previous simulations. Six different values of the weighting factors have been tested in the simulation for performance analysis. For the Kalman filter based localisation approaches, the two noise covariance matrices have the great impact on the localisation performance. When with smaller process noise covariance matrix and larger measurement noise covariance matrix, more trust will be given to the state prediction process. On the contrary, the localisation performance will more rely on the observation correction process. With the adaptively estimated noise covariance matrices, the proportion between these two matrices can be decided. However, the frequent changing estimation results for these two noise covariance matrices may lead to the filtering divergence. Thus, the two weighting factors plus with the offline value for these two noise covariance matrices have been added in the estimation process. In the simulation, if the different values of the two weighting factors α and β are selected, the proportion between these two noise covariance matrices will be changed in comparison with the estimated results. Therefore, the values for the two weighting factors α and β are always set as the same in the simulation. The purpose is to keep the same proportion level for these two noise covariance matrices for the application scenarios under consideration. The eCDF for each and the detailed localisation results have been given in Fig. 4 and Table IV.

Apparently, the same conclusion in comparison with the previous discussion can be made. With the smaller weighting factors (0.01, 0.05), the performance degradation with

TABLE IV
SIMULATION RESULTS WITH DIFFERENT WEIGHTING FACTORS

α, β	Median Error (m)	95^{th} Error (m)	STD (m)
$\alpha = \beta = 0.01$	0.025	0.064	0.018
$\alpha = \beta = 0.05$	0.022	0.051	0.016
$\alpha = \beta = 0.1$	**0.018**	**0.040**	**0.014**
$\alpha = \beta = 0.2$	0.020	0.041	0.014
$\alpha = \beta = 0.3$	0.019	0.043	0.015
$\alpha = \beta = 0.4$	0.021	0.050	0.015

the median error, 95^{th} error and average STD larger than 0.022m, 0.051m and 0.016m can be observed, when being compared with the localisation results for relatively larger weighting factors. This is caused by the reduction of the adaptive ability for the proposed algorithm. Alone with the increasing of the weighting factors, the adaptive ability for the proposed algorithm can be elevated, which can be proved by the localisation results with the weighting factors equal to 0.1, 0.2 and 0.3. However, with much more changes for the estimation of the noise covariance matrices, the stability of the filter maybe influenced, which may lead to the performance degradation or even the filtering divergence. The performance degradation can be discovered through the localisation results with 0.4 weighting factors. Meanwhile, the simulations with larger weighting factors (0.5-0.9) have also been conducted to comprehensively analyse the proposed algorithm. When being with these weighting factors, the filtering divergence can be observed during the flight of UAV in the simulation environment. This phenomenon is particularly significant at the position where UAV suddenly changed its position such as taking off or landing. This filtering divergence will directly lead to the position lost of it. Considering the focused applications, the primary objective is to prevent any positioning failure and performance oscillation. Thus, according to the simulation results, the weighting factors equal to 0.1 is selected since the best positioning performance in accuracy and precision can be achieved to keep the stability of the UAV and improve the inspection efficiency in that extremely confined space. Furthermore, considering $\boldsymbol{R}_i$ is estimated through a subtraction of two positive definite matrices, thus it might become negative after a new update process. To prevent this, if a negative estimation of $\boldsymbol{R}_i$ is calculated in this round, the weighting factor α will be directly set to zero. This means that the measurement noise covariance matrix in this round will be $\boldsymbol{R}_{off}$. Finally, throughout the calculated noise matrices $\boldsymbol{Q}_i$ and $\boldsymbol{R}_i$, the localisation performance can be improved.

IV. EXPERIMENTS

In this section, the description for a large number of experiments including laboratory experiments and field tests in the oil and gas pressure vessel will be given to comprehensively validate the proposed localisation algorithm and prove the effectiveness of the UAV autonomous inspection system.

A. Laboratory experiment

1) Environment setup: In order to exhaustively validate the performance of the proposed sensor fusion based algorithm for UAV positioning, the ground truth is required. In the laboratory experiment, considering the sub-millimeter accuracy, the OptiTrack V120:Trio [34] is utilised as the reference system to provide the ground truth for performance evaluation. Our experiment is performed in a confined area (1.95m $\times$ 3.0m $\times$ 2.3m) to mock the operational environment inside the oil and gas pressure vessel. All the anchor nodes are deployed on the same plane (X-Z plane) with the same distribution in field tests to suppose that these nodes can only be deployed near the entrance of the pressure vessel. This is to conform that anchor nodes in the system can be deployed without human entering the pressure vessel to aid the deployment. The laboratory experiment environment with anchor node distribution, coordinates of anchor nodes, the reference system and the UAV system have all been illustrated in Fig. 5.

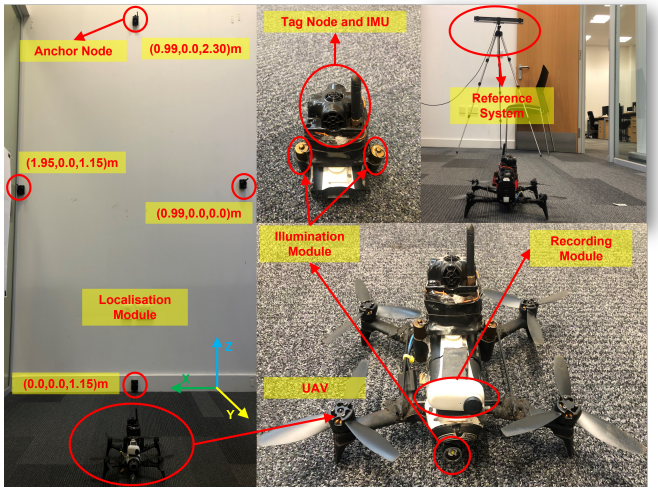

Fig. 5. Laboratory experiment environment.

2) UAV flight test: In laboratory experiments, same as the simulations, the flight path of UAV is set as a reverse "S". Three different sensor fusion based approaches including the EKF algorithm in this paper, the EKF based approach proposed by Guo et al. [23] and the sensor fusion based approach presented in [24] are compared with the proposed algorithm to prove the effectiveness of it. For all the aforementioned sensor fusion approaches, the STD of the measurement noise from the IMU module and the ultrasonic sensor nodes are assumed as 0.3m/s^2 and 0.01m. These are estimated with the measured acceleration and ranging information at fixed points and adjusted manually through trial and error. The threshold value for the virtual observation process and the sampling number for the estimation of noise covariance matrices are set as 5 and 50, respectively. With the existing reference system, the RMSE and eCDF have all been calculated and provided to validate the localisation performance. Here it needs to note that, due to the low position update rate for the ultrasonic based system and the unreasonable values for the ranging information, the huge localisation performance oscillation for the pure ultrasonic based approach and the sensor fusion based approaches without the virtual observation process always exists. This performance oscillation will directly lead to the UAV crash in this confined space, according to the experiments.

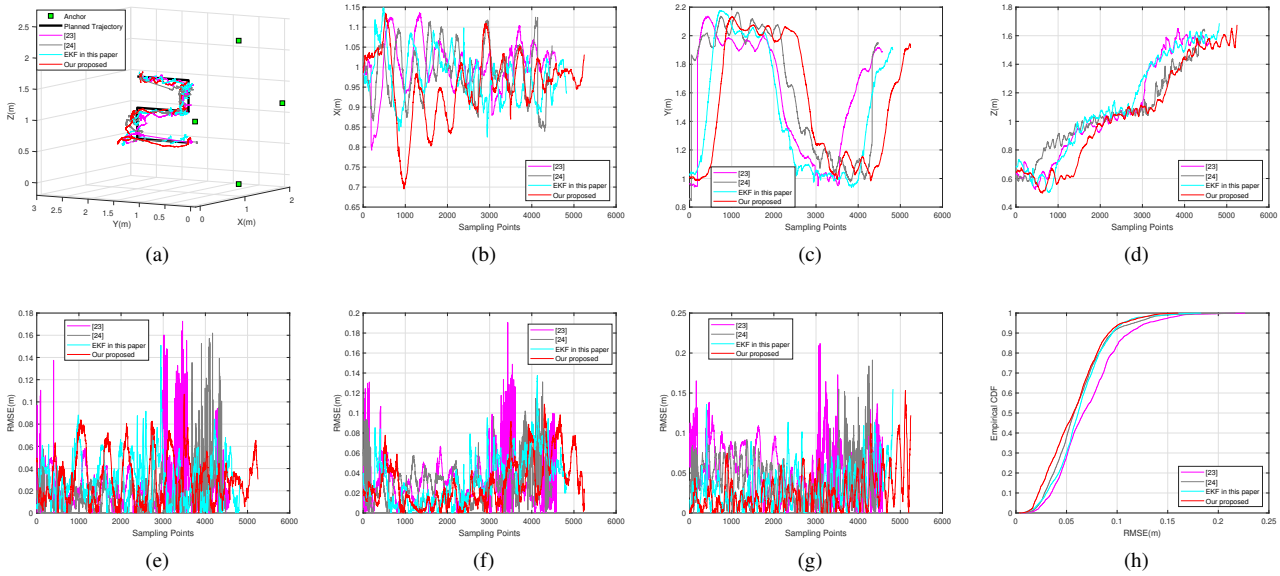

Fig. 6. Flight test results in the laboratory environment. (a) Flight trajectories results. (b) Flight trajectories in X direction. (c) Flight trajectories in Y direction. (d) Flight trajectories in Z direction. (e) Localisation error (m) in X direction. (f) Localisation error (m) in Y direction. (g) Localisation error (m) in Z direction. (h) eCDF results.

TABLE V
LOCALISATION PERFORMANCE FOR SENSOR FUSION BASED APPROACHES

Algorithm	Median Error (m)	95^{th} Error (m)	STD (m)	Update Rate (Hz)	Initialisation Time (s)
[23] with virtual observation	0.067	0.131	0.032	117	14.17
[24] with virtual observation	0.057	0.117	0.029	75	14.91
EKF in this paper with virtual observation	0.061	0.105	0.026	**118**	**10.07**
Our proposed	**0.056**	**0.104**	**0.026**	115	20.47

Thus, only the positioning results for these sensor fusion based approaches with the virtual observation process are provided.

As shown in Fig. 6 and Table V, the flight test results and localisation performance for the sensor fusion based approaches on UAV positioning in the laboratory environment have been given. In [23] and [24], two additional methods including the measurement calibration and outlier detection methods are proposed and added in the estimation process to deal with the performance oscillation issue led by the unreasonable value in the measured ranging information. Throughout these two additional methods, plus with the virtual observation process, the low update rate and performance oscillation issues can be eliminated with the median error, 95^{th} error and average STD up to 0.067m, 0.131m and 0.032m in such environment. Especially for the sensor fusion based approach in [24], with the added angular rate in the prediction process, the median error is further reduced to 0.057m. Nevertheless, the requirement of the suitable calibration parameters still limits and influences the performance of these. Some reference points with known position are desired help for the calculation of these parameters, which is difficult to achieve in the pressure vessel environments. The unsuitable parameters may even cause the over correction of the ranging measurements, this can be proved through the comparison of these two approaches with the EKF approach in this paper. From the localisation results, it can be observed that the median error for these are almost the same as with the EKF approach in this paper. Particularly, the approach proposed by Li et al. [24] even holds the better median error 0.057m. However, a huge performance degradation can be discovered with the 95^{th} error dropped to 0.117m and 0.131m. When being compared all these three approaches with the proposed method, the proposed method holds the best positioning performance in all of these three indexes with 0.056m median error, 0.104m 95^{th} error and 0.026m average STD. The performance for these approaches is restricted by the unknown and constant noise covariance matrices. When being with the constant noise covariance matrices, the system can hold the current status with stable performance which means high precision. Yet, the system cannot catch up the changes of the noise which may lead to the accuracy drop-off. This can also be discovered through the localisation results, that the EKF approach in this paper can attain the same average STD with the proposed algorithm. However, the drop-off for the median error can still be observed. Furthermore, the current noise model exploited for these three approaches are estimated by the acceleration and ranging information measured at fixed points with known position and adjusted manually through trial and error. This takes lots of time and is hard to achieve in the pressure vessel environments. Thus, the proposed approach is more suitable for the focused application

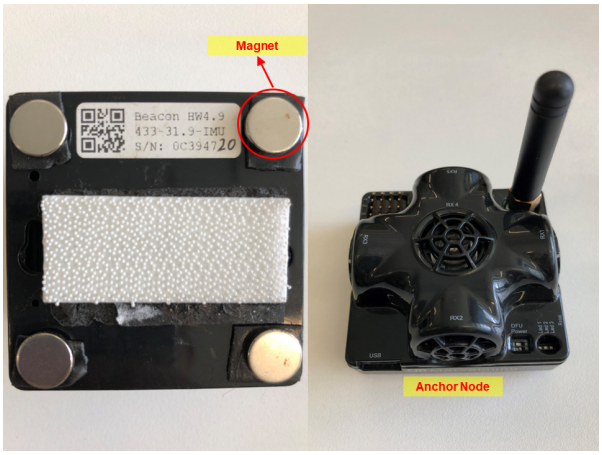

Fig. 7. Anchor node utilised in the oil and gas pressure vessel.

where it is difficult to measure or adjust the noise matrices.

Excluding the localisation accuracy and precision, the update rate or the computational complexity of the system and the algorithm also has great impact on the stability of UAV and the inspection performance [21]. As shown in Table V, the update rate for the position information and the initialisation time of each algorithm are provided. Clearly, the EKF approach in this paper holds the best update rate 118Hz due to its lowest complexity. However, a high update rate (115Hz) can still be obtained for the proposed algorithm. The initialisation time for these approaches including the initialisation of the ultrasonic system, the estimation of the original position of the UAV and the calculation of the offline data for the noise covariance matrices. Obviously, the EKF approach in this paper still holds the shortest initialisation time 10.07s, and the proposed algorithm holds the longest initialisation time 20.47s. This is caused by the calculation of the offline data for the noise covariance matrices. Additional 50 rounds estimation are required to capture sufficient data for more accurate calculation of the offline noise covariance matrices. Here it needs to note that, the initialisation time for the system is mostly determined by the update rate of the ultrasonic ranging information (the original position of the UAV is calculated through 50 position information estimated by the pure ultrasonic approach with the ranging information) and has no influence on the position update rate during the flight of UAV. Therefore, despite the proposed algorithm holds the longest initialisation time, it has no impact on the localisation performance and the inspection quality and efficiency of the system.

B. Flight test in the pressure vessel

Finally, in order to verify the effectiveness of the UAV based autonomous inspection system in the oil and gas pressure vessels, the flight tests in such environment have been carried out. Therein, the flight tests are only performed with the proposed approach, considering the unknown and difficult to adjust noise covariance matrices for other three approaches. Besides, due to the difficulty to measure the ground truth in such environment, only the flight trajectory is provided. Through the magnets attached on the anchor nodes as shown

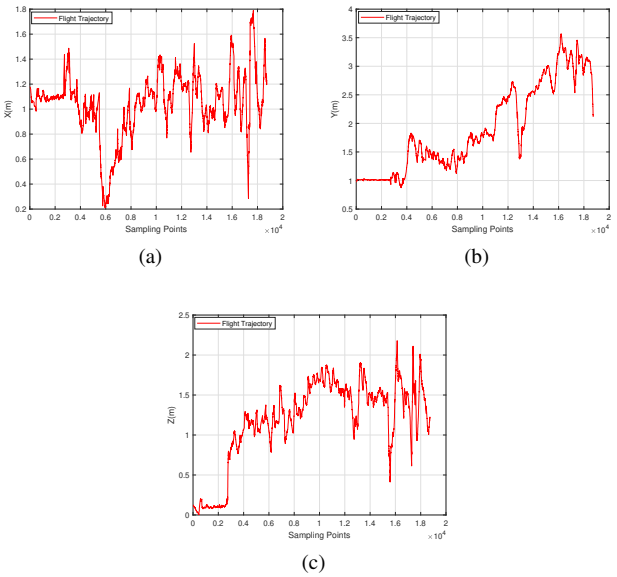

Fig. 8. Flight trajectory in field tests. (a) Flight trajectory in X direction. (b) Flight trajectory in Y direction. (c) Flight trajectory in Z direction.

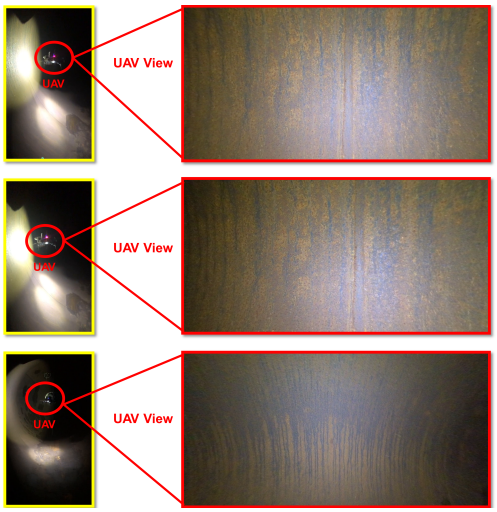

Fig. 9. Experiment snapshots for field tests.

in Fig. 7, the anchor nodes can be absorbed on the wall of the oil and gas pressure vessel near its entrance with the same distribution as in the laboratory experiment without human access. During the test, the UAV was flying inside the pressure vessel autonomously to capture images and recording video for the inspection of the corrosion on the surface.

As shown in Fig. 8 and Fig. 9, the flight trajectory in each direction and images captured by the UAV during the flight test have been depicted. Apparently, with the sensor fusion based localisation algorithm, the attached recording module and illumination module, high quality images with the resolution of 2560 $\times$ 1440 can be captured by the UAV system to identify the corrosion in that dark environment. In conclusion, the proposed ultrasonic and IMU based UAV autonomous inspection system is feasible for the focused applications to achieve the low cost autonomous inspection

in oil and gas pressure vessels.

V. Conclusion

Due to the increasing demands on the UAV autonomous inspection in the oil and gas industry, this article has proposed a low cost ultrasonic and IMU based UAV autonomous inspection system for the autonomous inspection inside oil and gas pressure vessels. In the beginning, the system overview was presented to provide a detailed information about each module in the system and the system operational process. Followed by, a comprehensive description for the proposed sensor fusion based approach including the EKF based approach, the AEKF based approach and the virtual observation process was given. The proposed approach was utilised to achieve the reliable, accurate, high position update rate and low computational complexity localisation of UAV in such environments. Finally, exhaustive simulations and experiments including laboratory experiments and field tests have been carried out to prove the effectiveness of the proposed algorithm and the developed system. Accordingly, high accuracy and precision localisation of UAV can be attained with the median localisation error, 95^{th} error and average STD to be 0.056m, 0.104m and 0.026m, respectively. Meanwhile, the position update rate for the system is significantly improved to 115Hz. Throughout these, it can be demonstrated that our proposed algorithm and system are feasible for the UAV autonomous inspection in oil and gas pressure vessels.

However, it requires to be noticed that the limitation for the proposed approach and system still exists. The long-term unavailability and low update rate of the observation information still has the impact on the localisation performance of the system due to the accumulation error from the prediction process. To deal with the existing problem, the multi-rate sampling updating can be a potential candidate, which will be the future research direction.

Acknowledgments

This article is fully supported by Research Excellence Award studentship from University of Strathclyde, partly supported by Low Cost Intelligent UAV Swarming Technology for Visual Inspection project from the UK Net Zero Technology Centre (Grant No. AI-P-028) and the MOEA/D-PPR research project (Grant No. IEC-NSFC-211434) funded by the Royal Society. The authors would also like to thank the Net Zero Technology Centre robotics team at the University of Strathclyde for their kindly support especially Dr Gordon Dobie, Dr Charles MacLeod, Mr Mark Robertson and Prof Xiutian Yan.

References

[1] H.-M. Chung, S. Maharjan, Y. Zhang, F. Eliassen, and K. Strunz, "Placement and routing optimization for automated inspection with unmanned aerial vehicles: A study in offshore wind farm," *IEEE Trans. Ind. Informat.*, vol. 17, no. 5, pp. 3032–3043, 2020.

[2] Z. Zhou, C. Zhang, C. Xu, F. Xiong, Y. Zhang, and T. Umer, "Energy-efficient industrial internet of uavs for power line inspection in smart grid," *IEEE Trans. Ind. Informat.*, vol. 14, no. 6, pp. 2705–2714, 2018.

[3] L. Yu, E. Yang, P. Ren, C. Luo, G. Dobie, D. Gu, and X. Yan, "Inspection robots in oil and gas industry: a review of current solutions and future trends," in *Proc. IEEE 25th Int. Conf. Automat. Comput.*, 2019, pp. 1–6.

[4] R. La Scalea, M. Rodrigues, D. P. M. Osorio, C. Lima, R. D. Souza, H. Alves, and K. C. Branco, "Opportunities for autonomous uav in harsh environments," in *Proc. 16th Int. Symp. Wireless Commun. Syst.*, 2019, pp. 227–232.

[5] Flyability. Elios 2—Indoor Drone for Confined Space Inspections. [Online]. Available: https://www.flyability.com/elios-2

[6] J. Nikolic, M. Burri, J. Rehder, S. Leutenegger, C. Huerzeler, and R. Siegwart, "A uav system for inspection of industrial facilities," in *Proc. IEEE Aerosp. Conf. Proc.*, 2013, pp. 1–8.

[7] S. S. Mansouri, C. Kanellakis, G. Georgoulas, and G. Nikolakopoulos, "Towards mav navigation in underground mine using deep learning," in *Proc. IEEE Int. Conf. Robot. Biomimetics*, 2018, pp. 880–885.

[8] C. Kanellakis, P. S. Karvelis, S. S. Mansouri, A.-A. Agha-Mohammadi, and G. Nikolakopoulos, "Towards autonomous aerial scouting using multi-rotors in subterranean tunnel navigation," *IEEE Access.*, vol. 9, pp. 66 477–66 485, 2021.

[9] P. Petráček, V. Krátkỳ, and M. Saska, "Dronument: System for reliable deployment of micro aerial vehicles in dark areas of large historical monuments," *IEEE Robot. Autom. Lett.*, vol. 5, no. 2, pp. 2078–2085, 2020.

[10] T. Özaslan, G. Loianno, J. Keller, C. J. Taylor, V. Kumar, J. M. Wozencraft, and T. Hood, "Autonomous navigation and mapping for inspection of penstocks and tunnels with mavs," *IEEE Robot. Autom. Lett.*, vol. 2, no. 3, pp. 1740–1747, 2017.

[11] T. Özaslan, G. Loianno, J. Keller, C. J. Taylor, and V. Kumar, "Spatio-temporally smooth local mapping and state estimation inside generalized cylinders with micro aerial vehicles," *IEEE Robot. Autom. Lett.*, vol. 3, no. 4, pp. 4209–4216, 2018.

[12] S. S. Mansouri, C. Kanellakis, D. Kominiak, and G. Nikolakopoulos, "Deploying mavs for autonomous navigation in dark underground mine environments," *Robot. Auton. Syst.*, vol. 126, p. 103472, 2020.

[13] M. Liu, L. Cheng, K. Qian, J. Wang, J. Wang, and Y. Liu, "Indoor acoustic localization: A survey," *Hum.-Centric Comput. Inf. Sci.*, vol. 10, no. 1, pp. 1–24, 2020.

[14] R. Watson, M. Kamel, D. Zhang, G. Dobie, C. MacLeod, S. G. Pierce, and J. Nieto, "Dry coupled ultrasonic non-destructive evaluation using an over-actuated unmanned aerial vehicle," *IEEE Trans. Autom. Sci. Eng.*, 2021.

[15] L. M. González-deSantos, J. Martínez-Sánchez, H. González-Jorge, F. Navarro-Medina, and P. Arias, "Uav payload with collision mitigation for contact inspection," *Autom. Construct.*, vol. 115, p. 103200, 2020.

[16] N. Gageik, P. Benz, and S. Montenegro, "Obstacle detection and collision avoidance for a uav with complementary low-cost sensors," *IEEE Access.*, vol. 3, pp. 599–609, 2015.

[17] Marvelmind. Precise (±2cm) Indoor Positioning and Navigation for autonomous robots, drones, vehicles and humans. [Online]. Available: https://www.marvelmind.com/

[18] D. Kang and Y.-J. Cha, "Autonomous uavs for structural health monitoring using deep learning and an ultrasonic beacon system with geo-tagging," *Comput. Aided Civil Infrastruct. Eng.*, vol. 33, no. 10, pp. 885–902, 2018.

[19] Y. Li, M. Scanavino, E. Capello, F. Dabbene, G. Guglieri, and A. Vilardi, "A novel distributed architecture for uav indoor navigation," *Transport. Res. Procedia.*, vol. 35, pp. 13–22, 2018.

[20] S. Zahran, A. M. Moussa, A. B. Sesay, and N. El-Sheimy, "A new velocity meter based on hall effect sensors for uav indoor navigation," *IEEE Sensors J.*, vol. 19, no. 8, pp. 3067–3076, 2018.

[21] B. Yang and E. Yang, "A survey on radio frequency based precise localisation technology for uav in gps-denied environment," *J. Intell. Robot. Syst.*, vol. 103, no. 3, pp. 1–30, 2021.

[22] D. Feng, C. Wang, C. He, Y. Zhuang, and X.-G. Xia, "Kalman-filter-based integration of imu and uwb for high-accuracy indoor positioning and navigation," *IEEE Internet Things J.*, vol. 7, no. 4, pp. 3133–3146, 2020.

[23] K. Guo, Z. Qiu, C. Miao, A. H. Zaini, C.-L. Chen, W. Meng, and L. Xie, "Ultra-wideband-based localization for quadcopter navigation," *Unmanned Syst.*, vol. 4, no. 01, pp. 23–34, 2016.

[24] M.-G. Li, H. Zhu, S.-Z. You, and C.-Q. Tang, "Uwb-based localization system aided with inertial sensor for underground coal mine applications," *IEEE Sensors J.*, vol. 20, no. 12, pp. 6652–6669, 2020.

[25] X. Li and Q. Xu, "A reliable fusion positioning strategy for land vehicles in gps-denied environments based on low-cost sensors," *IEEE Trans. Ind. Electron.*, vol. 64, no. 4, pp. 3205–3215, 2016.

[26] C. Shen, Y. Zhang, X. Guo, X. Chen, H. Cao, J. Tang, J. Li, and J. Liu, "Seamless gps/inertial navigation system based on self-learning square-root cubature kalman filter," *IEEE Trans. Ind. Electron.*, vol. 68, no. 1, pp. 499–508, 2020.

[27] M. Song, R. Astroza, H. Ebrahimian, B. Moaveni, and C. Papadimitriou, "Adaptive kalman filters for nonlinear finite element model updating," *Mech. Syst. Signal Process.*, vol. 143, p. 106837, 2020.
[28] Y. Huang, Y. Zhang, B. Xu, Z. Wu, and J. A. Chambers, "A new adaptive extended kalman filter for cooperative localization," *IEEE Trans. Aerosp. Electron. Syst.*, vol. 54, no. 1, pp. 353–368, 2017.
[29] B. Zheng, P. Fu, B. Li, and X. Yuan, "A robust adaptive unscented kalman filter for nonlinear estimation with uncertain noise covariance," *Sensors*, vol. 18, no. 3, p. 808, 2018.
[30] Y. Qin, H. Duan, and J. Han, "Direct inverse hysteresis compensation of piezoelectric actuators using adaptive kalman filter," *IEEE Trans. Ind. Electron.*, vol. 69, no. 9, pp. 9385–9395, 2021.
[31] A. Mohamed and K. Schwarz, "Adaptive kalman filtering for ins/gps," *J. Geodesy.*, vol. 73, no. 4, pp. 193–203, 1999.
[32] F. Jiancheng and Y. Sheng, "Study on innovation adaptive ekf for in-flight alignment of airborne pos," *IEEE Trans. Instrum. Meas.*, vol. 60, no. 4, pp. 1378–1388, 2011.
[33] S. Akhlaghi, N. Zhou, and Z. Huang, "Adaptive adjustment of noise covariance in kalman filter for dynamic state estimation," in *Proc. IEEE Power Energy Soc. Gen. Meeting.*, 2017, pp. 1–5.
[34] OptiTrack. OptiTrack V120:Trio Data Sheet. [Online]. Available: https://www.optitrack.com/cameras/v120-trio/

Beiya Yang (Graduate Student Member, IEEE) received the B.Eng. degree in Electronic Information Engineering from Northwestern Polytechnical University, Xi'an, China, in 2013 and the M.Sc degree in Information and Communication Engineering from National University of Defense Technology, Changsha, China, in 2015. He is currently pursuing the Ph.D. degree in high-precision UAV positioning for autonomous inspection, with the Department of Design, Manufacturing and Engineering Management (DMEM) at University of Strathclyde, Glasgow, UK, since 2019. His current research interests include indoor localisation technology, unmanned aerial vehicles (UAV) localisation and wireless sensor networks.

Erfu Yang (Senior Member, IEEE) received his Ph.D. degree in Robotics from the School of Computer Science and Electronic Engineering, University of Essex, Colchester, UK, in 2008. He is currently a Senior Lecturer in the Department of Design, Manufacturing and Engineering Management (DMEM), University of Strathclyde, Glasgow, UK. His main research interests include robotics, autonomous systems, mechatronics, manufacturing automation, signal and image processing, computer vision and applications of machine learning and artificial intelligence, etc. He has over 160 publications in these areas, including more than 80 journal papers and 10 book chapters. Dr. Yang has been awarded over 15 research grants as PI (principal investigator) or CI (co-investigator). He is the Fellow of the UK Higher Education Academy, Member of the UK Engineering Professors' Council, Senior Member of the IEEE Society of Robotics and Automation, IEEE Control Systems Society, Publicity Co-Chair of the IEEE UK and Ireland Industry Applications Chapter, Committee Member of the IET SCOTLAND Manufacturing Technical Network. He is also an associate editor for the Cognitive Computation journal published by Springer.

Leijian Yu (Graduate Student Member, IEEE) received the B.Eng. degree in electrical information engineering and the M.Sc degree in information and communication engineering from China University of Petroleum (East China), Qingdao, China, in 2015 and 2018, respectively. He is currently pursuing the Ph.D. degree in robotics and autonomous systems for asset visual inspection, with the Department of Design, Manufacturing and Engineering Management (DMEM) at the University of Strathclyde, Glasgow, UK, since 2018. His current research interests include machine learning with applications on unmanned aerial vehicles (UAV), UAV vision-based autonomous navigation and image contrast enhancement.

Cong Niu (Member, IEEE) has been awarded the B.Eng. with Honours, degree of Electronic Engineering from University of Central Lancashire, Preston, UK in 2014. Then awarded with the M.Sc degree on Embedded Digital System from University of Sussex, Brighton, UK in 2015. He received his Ph.D. degree in robotics and autonomous systems for agriculture applications, from the Department of Design, Manufacturing and Engineering Management (DMEM), University of Strathclyde, Glasgow, UK, in 2021. He is currently working as a Research Associate in DMEM for the project of "Made Smarter Innovation Research Centre for Smart, Collaborative Industrial Robotics". His current research interests include field and indoor path planning, modeling and simulation, unmanned ground and aerial vehicles, smart factory and collaborative robotics.